Key Engineering Materials
ISSN: 1662-9795, Vol. 926, pp 1093-1099
doi:10.4028/p-cva3h4

Submitted: 2021-12-22
Revised: 2022-01-13
Accepted: 2022-02-04
Online: 2022-07-22

Characterization of Yield Surface Evolution of AZ31 from Shear to Equibiaxial Tension

LOU Yanshan[1,a*], ZHANG Jia[1,b], ZHANG Chong[1,c] and YOON Jeong Whan[2,d]

[1]Xi'an Jiaotong University, China

[2]KAIST, South Korea

[a]ys.lou@xjtu.edu.cn, [b]MES1001zj@stu.xjtu.edu.cn, [c]rushzc@stu.xjtu.edu.cn, [d]j.yoon@kaist.ac.kr

Keywords: Sheet metal forming, Yield function, Yield surface evolution, anisotropic hardening, magnesium alloy

Abstract. This research characterized the strain hardening behavior of AZ31 under different stress states from shear to balanced biaxial tension with a newly proposed yield function. Experiments are conducted for AZ31 magnesium alloy by in-plane shear specimens, dogbone specimens, notched specimens and bulging specimens to characterize the flow behavior under different stress states. The flow behaviors are characterized by a newly proposed yield function in a form of the three stress invariants. The proposed yield function is implemented into ABAQUS/Explicit to predict the plastic response of the alloy under different stress states. It is shown that the proposed yield function can precisely predict the distinct flow behaviors and reaction forces from shear to equibiaxial tension from the initial yielding to fracture.

Introduction

Magnesium alloys are very important for lightweight design of structures because of its low density and good mechanical properties. However, the plastic behaviors of magnesium alloy are very complicated due to their complicated plastic deformation mechanisms of slip, twinning, detwinning etc. Most magnesium alloys show strong anisotropy in strength, obvious strength differential effect between tension and compression and very distinct strain hardening behaviors at different loading conditions. The complicated plastic behaviors are big challenges for analytical and numerical analysis and design of magnesium components.

To model the anisotropic behaviors of sheet metals, many yield functions were proposed, such as Hill48, Yld89 [1], Yld91 [2], Yld2000-2d [3], Yld2004-18p [4], anisotropic Drucker [5], rYld2004 [6], BBC families [7-8], Aretz-Barlat [9], Yoshida et al. [10] and Cazacu [11]. Many asymmetric yield functions were introduced to characterize the strength differential (SD) effect of hexagonal-close packed (HCP) metals. These asymmetric yield functions include Cazacu-Barlat'2004 [12], CPB'2006 [13], pYld2000-2d [14], Yoon'2014 [15], Hu et al. [16]. In the last decade, anisotropic hardening behaviors are increasingly modelled, such as Stoughton-Yoon'2009 [17], CQN [18], Pack et al. [19], Hu et al. [20-22], Chen et al. [23]. All the yield functions proposed above greatly improve the modelling accuracy of plastic deformation in metal forming processes. However, the stress states considered by the above functions are generally uniaxial tension, equibiaxial tension and uniaxial compression. Shear and plane strain tension are rarely considered together in analytical modelling except the pDrucker yield function [24].

In this research, experiments are conducted for AZ31 from shear to equibiaxial tension by in-plane shear specimens, dogbone specimens, notched specimens and bulging tests. The flow curves are obtained at different stress states of shear, uniaxial tension, plane strain tension and equibiaxial tension. Strength anisotropy is compared with the effect of stress states on strain hardening behaviors. The much more apparent effect of stress states on strain hardening is modelled by a newly proposed yield function. The predicted flow curves under these four stress states are compared with experimental results to investigate the performance of the proposed yield function. Numerical simulations are conducted for the notched and shear specimens. The predicting accuracy is further investigated by comparing the reaction force between simulation and experiments.

Experiments

In this study, a magnesium alloy AZ31 were tested under quasi-static loading conditions. The thickness of the specimen is 1.1 mm. The tests were designed at four stress states of shear, uniaxial tension, plane strain tension and equibaxial tension by the specimens in Fig. 1 (a) dogbone specimen, (b) in-plane shear, (c) notched specimens and (d) circular specimens for bulging tests. The shear specimen and notched specimen are modified compared to the original version [25, 26]. Experimental processes were recorded and analysed by the XTOP digital image correlation system.

Experiments were conducted for dogbone, notched and shear specimens along different loading directions to investigate the anisotropy in strength of the materials. The true stress-true strain curves from experiments are compared along different loading directions in Fig. 2 for AZ31 at uniaxial tension and shear. For uniaxial tension, it shows the strength of AZ31 along RD is obviously about 9% lower than the other six stretching directions. The strength anisotropy of AZ31 from 15° to 90° with respect to RD is less than 2.5% and negligible. For shear, it shows the strength anisotropy in shear is less than 4% for AZ31.

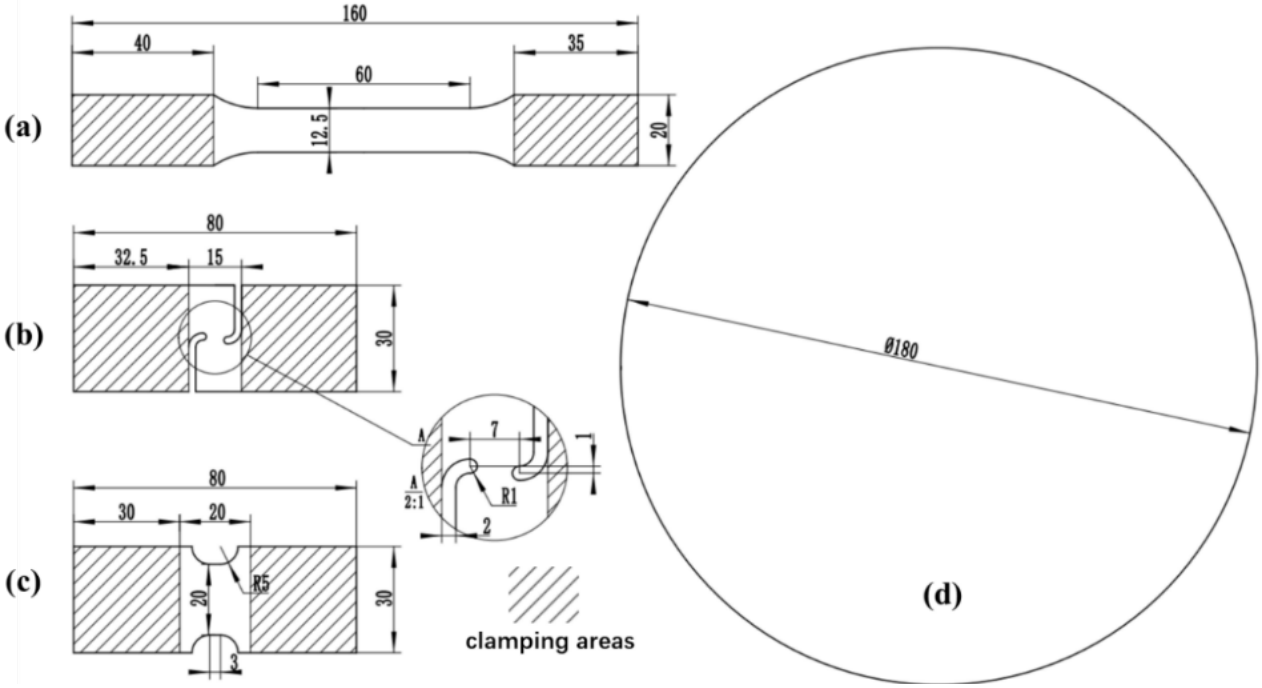

Fig. 1. Tested specimens: (a) dog-bone; (b) shear; (c) notched specimens for plane strain tension; (d) bulge specimen. The dimensions are in [mm].

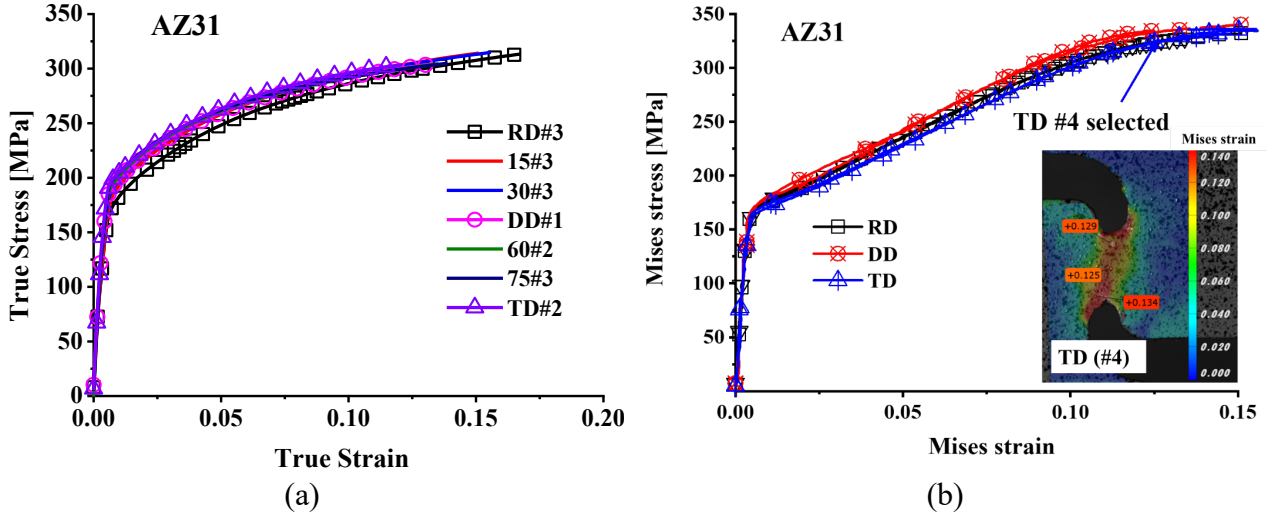

Fig. 2. Evaluation of strength anisotropy under (a) uniaxial tension and (b) shear.

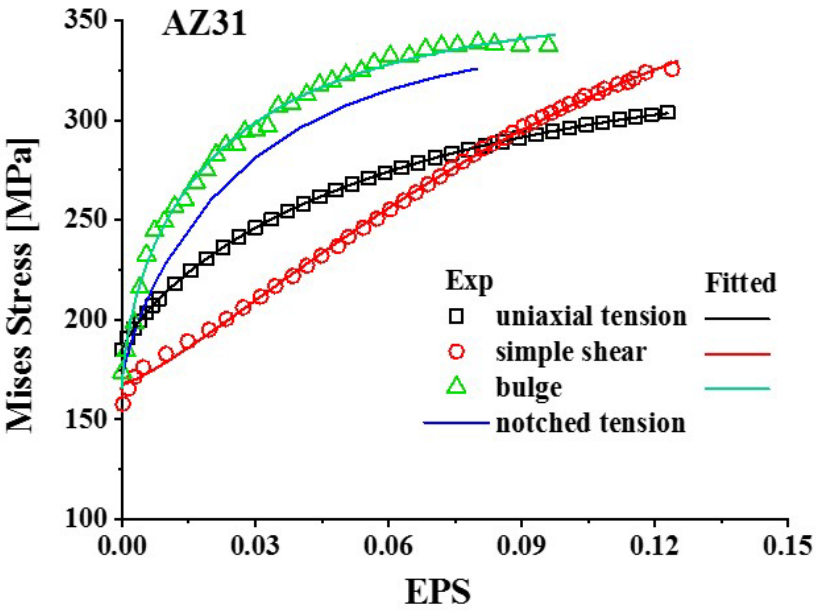

Fig. 3. Comparison of flow curves under the four different stress states for AZ31.

Table 1 The calibrated coefficients of the Hockett-Sherby hardening law ($\sigma = A - (A - B)exp(-C\bar{\varepsilon}^{p^n})$) as Eq. (26) for the tested materials under different stress states.

Materials	Stress states	coefficients				Fitted
		A [MPa]	B [MPa]	C	n	error (R^2)
AZ31	uniaxial tension	330	184	9.2	0.81	0.9999
	shear	395	160	17.4	1.27	0.9983
	plane strain tension	343	171	18.8	0.83	N/A
	equibiaxial tension	357.5	166.3	11.9	0.66	0.9922

The flow curves are compared for AZ31 under these four stress states in Fig. 3. The flow curves under plane strain tension and equibiaxial tension are much higher than that under uniaxial tension and shear. The slope of the flow curves under plane strain and equibiaxial tension is also higher than the other two stress states. The shear flow curve is the lowest when the strain is less than 0.075, but rises to be higher than the uniaxial tensile flow curves when the plastic strain is higher than 0.09. In addition, the strength anisotropy of AZ31 is about 9%. However, the maximum difference of the flow curves under these four stress states is larger than 30%, which is much more apparent than the strength anisotropy of AZ31. The complicated strain hardening behaviour indicates a severe change of the yield surface with respect to plastic strain under proportional loading for AZ31, which must be reasonably considered in the constitutive modelling of plastic deformation behaviors.

The experimental flow curves under the four different stress states were fitted by the Hockett-Sherby law as plotted in Fig. 3. The coefficients of the Hockett-Sherby hardening law are summarized in Table 1 for the tested materials under different stress states. The fitting R-squared values are all above 0.99 which shows a good fit for the test.

A Newly Proposed Yield Function

The distinct strain hardening behavior of AZ31 in Fig. 3 is modelled by a newly proposed yield function [27] as below:

$$f(\sigma_{ij}) = a\left\{bI_1 + \left[(J_2^3 - cJ_3^2)^{1/2} - dJ_3\right]^{1/3}\right\} \quad (1)$$

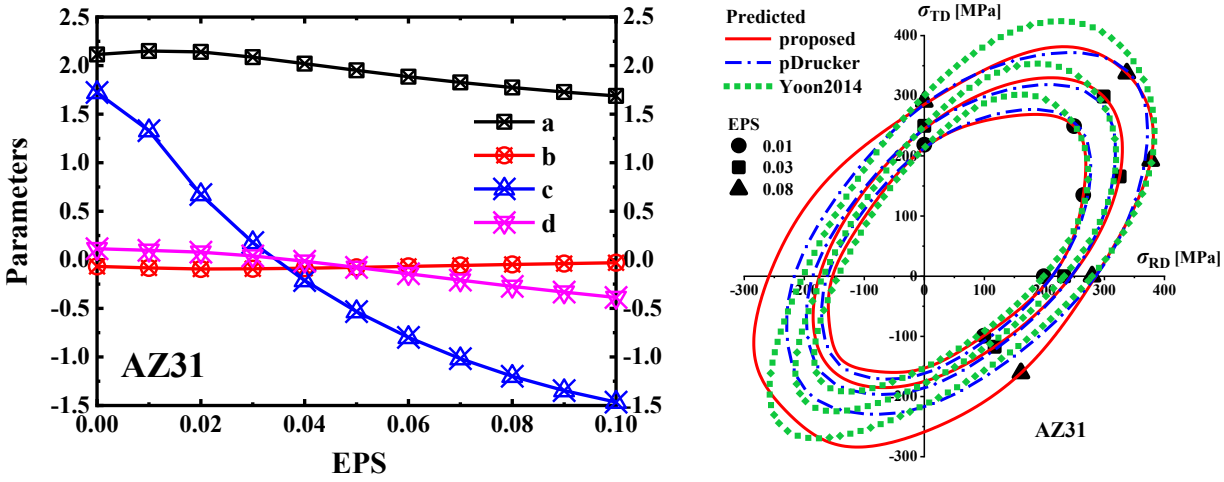

Fig. 4. Evolution of (a) the yield function parameters and (b) the yield surface.

where b considers the pressure effect, c and d model the influence of the third invariant J_3 on yielding with the even and asymmetric form, respectively. The parameter c adjusts the curvature of the yield surface. The parameter d considers the SD effect for pressure-insensitive materials. The proposed universal yield function can be easily reduced to other popular stress invariant-based functions, such as von Mises, Prager-Drucker, Drucker, Cazacu-Barlat'2004, Yoon'2014 and pDrucker. After transformation with a Lode and triaxiality dependent form with the derived equations [28, 29], the four parameters can be analytically computed by the yield stresses under shear, uniaxial tension, plane strain tension and equibiaxial tension as below:

$$\begin{cases} a = \dfrac{\sqrt{3}\bar{\sigma}_{UT}}{\bar{\sigma}_{Shear}} \\ b = \dfrac{1}{3}\left(\dfrac{\bar{\sigma}_{Shear}}{\bar{\sigma}_{PST}} - 1\right) \\ d = \dfrac{27}{4}\left[\left(\dfrac{\bar{\sigma}_{UT}}{a\bar{\sigma}_b} - 2b\right)^3 - \left(\dfrac{1}{a} - b\right)^3\right] \\ c = \dfrac{27 - \left[27\left(\frac{1}{a} - b\right)^3 + 2d\right]^2}{4} \end{cases} \tag{2}$$

Therefore, the parameters a, b, c and d of the proposed function are calculated at different plastic strain with its evolution as shown in Fig. 4. The yield surface evolution under different strain is also characterized as shown in the figure. It shows that the evolution of yield surface can be precisely modelled by the proposed yield function with its parameters computed by Eq. (2).

Numerical Simulations

The proposed yield function is applied into Abaqus/Explicit. First, simulations conducted with a single C3D8R element under these four stress states. The predicted Mises stress-strain curves for AZ31 are compared with the analytical ones computed by the Hockett-Sherby hardening law for the four stress states in Fig. 5. It is observed that the numerical prediction matches with the analytical computation with no obvious difference for the four loading conditions. The comparison demonstrates both the correct implementation of the proposed yield function in numerical simulation and the powerful predictability of the proposed yield function for severely different strain hardening behaviour under shear, uniaxial tension, plane strain tension and equibiaxal tension.

Numerical simulations are then conducted for the notched and shear specimens in Fig. 6 to predict the load responses. The predicting results are compared with the pDrucker function under isotropic hardening. The comparisons of the load-stroke curves between experiments and prediction by different yield functions for the notched tensile tests are plotted in Fig. 6 (a) for notched tensile tests and (b) for simple shear tests. It shows the proposed yield function have high accuracy to predict the

load response of notched tensile tests for AZ31 with the maximum error of about less than 1%. The maximum predicting errors of load response of simple shear tests are about 2.0% for AZ31 from the onset of plastic deformation to the onset of fracture during the tests. It is because the input is the strain hardening behaviour under four different stress states summarized in Table 1 which precisely characterize the strain hardening behaviour under these four stress states.

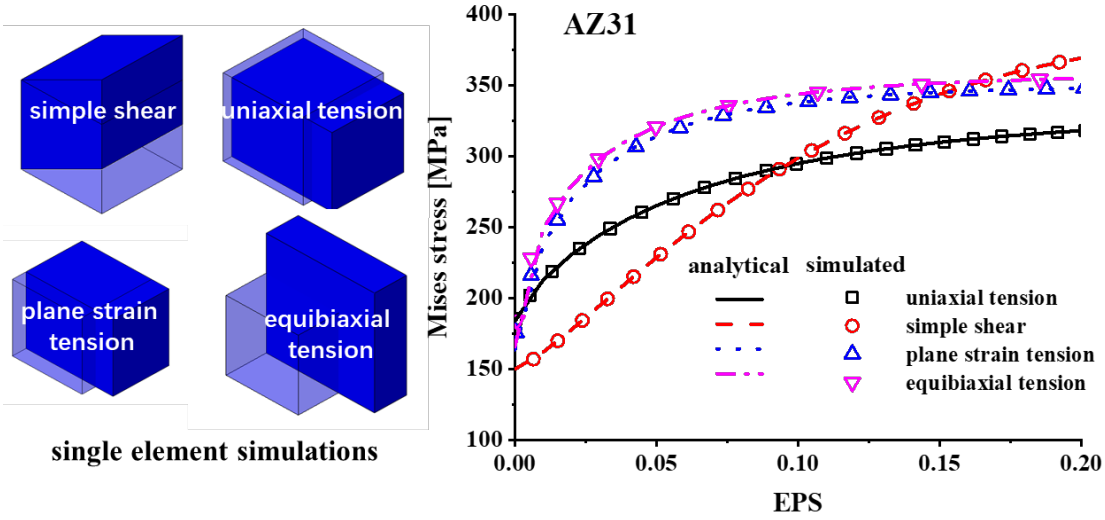

Fig. 5. Comparison of the Mises stress-EPS curves between simulation and analytical calculation under the four different stress states for AZ31.

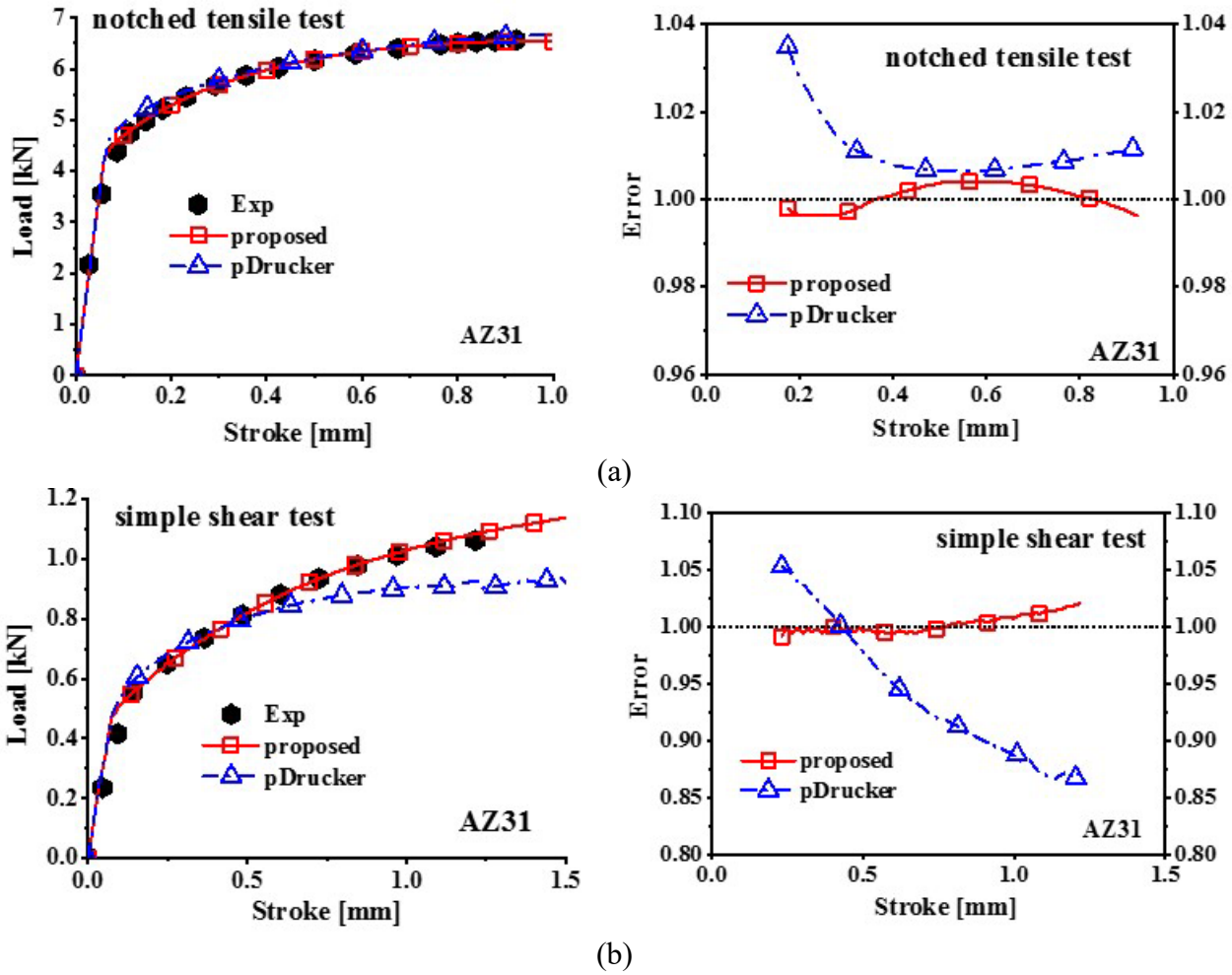

Fig. 6. Comparison of the Mises stress-EPS curves between simulation and analytical calculation under the four different stress states for AZ31.

Conclusions

This study characterizes the distinct strain hardening behavior of AZ31 under different stress states of shear, uniaxial tension, plane strain tension and equibiaxial tension by experiments, analytical modelling and numerical verification. The results show that the stress state effect is much more apparent than the strength anisotropy for the alloy. It also indicates that the proposed function can precisely model the strain hardening behavior under different stress states from yielding to fracture.

References

[1] F. Barlat, J. Lian, Plastic behavior and stretchability of sheet metals. Part I: Yield function for orthotropic sheets under plane stress conditions, Int. J. Plast. 5 (1989) 51–66.

[2] F. Barlat, D.J. Lege, J.C. Brem, A six-component yield function for anisotropic materials, Int. J. Plast. 7 (1991) 693–712.

[3] F. Barlat, J.C. Brem, J.W. Yoon, K. Chung, R.E. Dick, D.J. Lege, F. Pourboghrat, S.-H. Choi, E. Chu, Plane stress yield function for aluminum alloy sheet-part I: theory, Int. J. Plast. 19 (2003) 1297–1319.

[4] F. Barlat, H. Aretz, J.W. Yoon, M.E. Karabin, J.C. Brem, R.E. Dick, Linear transformation-based anisotropic yield functions, Int. J. Plast. 21 (2005) 1009–1039

[5] Y. Lou, J.W. Yoon, Anisotropic yield function based on stress invariants for BCC and FCC metals and its extension to ductile fracture criterion, Int. J. Plast. 101 (2018) 125–155.

[6] Y. Lou, S. Zhang, J.W. Yoon, A reduced Yld2004 function for modeling of anisotropic plastic deformation of metals under triaxial loading, Int. J. Mech. Sci. 161-162 (2019) 105027.

[7] D. Banabic, T. Kuwabara, T. Balan, D.S. Comsa, D. Julean, Non-quadratic yield criterion for orthotropic sheet metals under plane-stress conditions, Int. J. Mech. Sci. 45 (2003) 797–811.

[8] D. Banabic, H. Aretz, D.S. Comsa, L. Paraianu, An improved analytical description of orthotropy in metallic sheets, Int. J. Plast. 21 (2005) 493–512.

[9] H. Aretz, F. Barlat, New convex yield functions for orthotropic metal plasticity, Int. J. Non-Lin. Mech. 51 (2013) 97–111.

[10] F. Yoshida, H. Hamasaki, T. Uemori, A user-friendly 3D yield function to describe anisotropy of steel sheets, Int. J. Plast. 45 (2013) 119-139.

[11] O. Cazacu, New yield criteria for isotropic and textured metallic materials, Int. J. Solids Struct. 139 (2018) 200–210.

[12] O. Cazacu, F. Barlat, A criterion for description of anisotropy and yield differential effects in pressure-insensitive metals, Int. J. Plast. 20 (2004) 2027–2045.

[13] O. Cazacu, B. Plunkett, F. Barlat, Orthotropic yield criterion for hexagonal close packed metals, Int. J. Plast. 22 (2006) 1171–1194.

[14] Y. Lou, H. Huh, J.W. Yoon, Consideration of strength differential effect in sheet metals with symmetric yield functions, Int. J. Mech. Sci. 66 (2013) 214–223.

[15] J.W. Yoon, Y. Lou, J. Yoon, M.V. Glazoff, Asymmetric yield function based on the stress invariants for pressure sensitive metals, Int. J. Plast. 56 (2014) 184–202.

[16] Q. Hu, X. Li, X. Han, H. Li, J. Chen, A normalized stress invariant-based yield criterion: modeling and validation, Int. J. Plast. 99 (2017) 248-273.

[17] T.B. Stoughton, J.W. Yoon, Anisotropic hardening and non-associated flow in proportional loading of sheet metals, Int. J. Plast. 25 (2009) 1777–1817.

[18] E.-H. Lee, H. Choi, T.B. Stoughton, J.W. Yoon, Combined anisotropic and distortion hardening to describe directional response with Bauschinger effect, Int. J. Plast. 122 (2019) 73–88.

[19] N. Park, T.B. Stoughton, J.W. Yoon, A criterion for general description of anisotropic hardening considering strength differential effect with non-associated flow rule, Int. J. Plast. 121 (2019) 76–100.

[20] Q. Hu, J.W. Yoon, N. Manopulo, P. Hora, A coupled yield criterion for anisotropic hardening with analytical description under associated flow rule: Modeling and validation, Int. J. Plast. 136 (2021) 102882.

[21] Q. Hu, J.W. Yoon, Analytical description of an asymmetric yield function (Yoon2014) by considering anisotropic hardening under non-associated flow rule, Int. J. Plast. 140, (2021) 102978.

[22] Q. Hu, J.W. Yoon, T.B. Stoughton, Analytical determination of anisotropic parameters for Poly6 yield function, Int. J. Plast. 201 (2021) 106467.

[23] Z. Chen, Y. Wang, Y. Lou, User-friendly anisotropic hardening function with non-associated flow rule under the proportional loadings for BCC and FCC metals, Mech. Mat. (2022) doi.org/10.1016/j.mechmat.2021.104190.

[24] Y. Lou, S. Zhang, J.W. Yoon, Strength modeling of sheet metals from shear to plane strain tension, Int. J. Plast. 134 (2020) 102813.

[25] Y. Lou, H. Huh, Prediction of ductile fracture for advanced high strength steel with a new criterion: Experiments and simulation, J. Mater. Process. Technol. 213 (2013) 1284–1302.

[26] C. Zhang, Y. Lou, S. Zhang, T. Clausmeyer, A.E. Tekkaya, Q. Chen, Q. Zhang, Large strain flow curve identification for sheet metals under complex stress states, Mech. Mat. 161 (2021) 103997.

[27] Y. Lou, C. Zhang, S. Zhang, J.W. Yoon, S. Zhang, A general yield function with differential hardening for strength modelling from shear to equibiaxial tension, under review.

[28] Y. Lou, H. Huh, Extension of a shear-controlled ductile fracture model considering the stress triaxiality and the Lode parameter, Int. J. Solids Struct. 50 (2013) 447–455.

[29] Y. Lou, J.W. Yoon, H. Huh, Modeling of shear ductile fracture considering a changeable cut-off value for stress triaxiality, Int. J. Plast. 54, (2014) 56–80.